

# Velocity structures from sunspot statistics in cycles 10 to 22

## II. Latitudinal velocity and correlation functions

Pentti Pulkkinen<sup>1,2</sup> and Ilkka Tuominen<sup>2</sup>

<sup>1</sup> Department of Physics, Theory Division P.O. Box 9, FIN-00014, University of Helsinki, Finland

<sup>2</sup> Department of Geosciences and Astronomy, University of Oulu, P.O. Box 333, FIN-90571 Oulu, Finland

Received 11 July 1996 / Accepted 11 December 1997

**Abstract.** From sunspot observations between 1853-1996 we calculate latitudinal velocities and correlation functions — the Reynolds stress and the helicity. Latitudinal motions exist, but their behaviour is not certain. The Reynolds stress is strongly present but the helicity is negligible.

**Key words:** Sun: activity; photosphere; sunspots

---

### 1. Introduction

While the differential rotation is easy to find from sunspot observations, the latitudinal motion and the correlation between horizontal velocities are more difficult to measure, even qualitatively. For the covariance, or the horizontal Reynolds stress, its existence is usually accepted, but within large variations in magnitude. For the latitudinal motion the situation is more problematic – while some authors report on large mean latitudinal velocities, others claim their nonexistence.

J. Tuominen (1941) proposed that the mean latitudinal motion is poleward at high latitudes and equatorward at low latitudes suggesting two large convective circulation cells at both hemispheres. Although this behaviour has been confirmed afterwards by some authors (e.g. Howard and Gilman 1986), the statistical relevance of these measurements is not totally clear, see e.g. Ward (1973) and Balthasar et al. (1986) who found no significant latitudinal motion. Furthermore, J. Tuominen and Kyröläinen (1982), for recurrent sunspots, found a phase dependence for the latitudinal flow between activity minimum and maximum. J. Tuominen et al. (1983) discovered also that the latitude boundary (activity belt) separating poleward and equatorward flows was moving during the cycle. This phenomenon may be related to the torsional oscillation that was found by Howard and LaBonte (1980), (see also Rüdiger et al., 1986). Therefore the observed mean latitudinal motion may result both from hydrodynamic circulation and solar magnetic cycle.

*Send offprint requests to:* Pentti Pulkkinen

Ward (1965) discovered a large covariance for all sunspots from the Greenwich Photoheliographic Results (GPR) but Gilman & Howard (1984), using Mt. Wilson data, found it only for sunspot groups. Single spots had very small covariance and it was pointed out that the covariance of groups could partially result from their geometric changes during their life time. This assumption was supported by Nesme-Ribes et al. (1993), who found no significant Reynolds stress in their data.

### 2. Correlation functions

During the past decades we have learned that the solar differential rotation is not a fossil but is generated and continuously maintained by the angular momentum transport from higher latitudes toward the equator. Measurements from the GPR by Ward (1965) reveal the existence of this transport, mostly by the Reynolds stress. On the other hand, a theoretical approach for the origin of differential rotation, provided by Rüdiger (1980), addresses, apart from the Reynolds stress, meridional circulations and magnetic field as other possible sources of angular momentum transport.

#### 2.1. Reynolds stress

Since the discovery by Ward (1965) from sunspot observations it has been clear that the horizontal Reynolds stress  $Q_{\theta\phi} = \langle u'_\theta u'_\phi \rangle$  cannot be described by just the classical viscosity-type Boussinesq ansatz  $Q_{\theta\phi}^{(B)} = \nu_T(u'_{\theta,\phi} + u'_{\phi,\theta})$  with effective eddy viscosity  $\nu_T$ .<sup>1</sup> Firstly, it gives a wrong sign for  $Q_{\theta\phi}$  when compared with observations. Secondly, as pointed out by Rüdiger (1980), Reynolds stress is the main generator of the differential rotation and thus has to have a maintaining character rather than being diffusive. This means that  $Q_{\theta\phi}$  must be a function of not only of the gradients of rotation ( $\Omega$ ) but also of  $\Omega$  itself. Rüdiger's

---

<sup>1</sup> We denote the fluctuation field with a prime and the brackets indicate the mean value

formula describes this dependence ( $\Lambda$ -effect):

$$\frac{Q_{\theta\phi}}{\nu_T} = \left( -\frac{1}{\Omega} \frac{\partial\Omega}{\partial\theta} + H^{(1)} \cos\theta \sin\theta + H^{(2)} \cos\theta \sin^3\theta \right) \sin\theta\Omega. \quad (1)$$

The solar surface rotation rate is often written in the form

$$\Omega = A + B \cos^2\theta, \quad (2)$$

which can be installed into Eq. 1 and we obtain

$$Q_{\theta\phi} = \nu_T \Omega_* (w_1 + w_2 \sin^2\theta) \cos\theta \sin^2\theta, \quad (3)$$

where  $w_1 = H^{(1)} + 2B/\Omega_*$  and  $w_2 = H^{(2)} - BH^{(1)}/\Omega_*$  are and  $\Omega_* = A + B$  is the rotation rate at the poles.

The profile presented in Eq. 3 is in accordance with sunspot measurements (Ward, 1965; Gilman & Howard, 1984) and also is supported by numerical simulations (Pulkkinen et al., 1993) and other models (Canuto et al., 1994). For our work, a good comparison is provided by Paternò et al. (1991) who have analyzed the GPR. They found that the angular momentum flux is greater in the latitude band between 10 and 30 degrees than in the equatorial region, in accordance with the  $\Lambda$ -effect.

## 2.2. Helicity

Another correlation function, the helicity is also connected to the horizontal velocities. The helicity of the velocity field inside the solar convection zone would be of fundamental importance for understanding the solar dynamo action. The  $\alpha$ -tensor (Krause and Rädler, 1980), describing the dynamo effect is proportional to the helicity can be written, assuming axial symmetry and excluding small terms (with  $u'_r, u'_\theta \ll u'_\phi$ ):

$$\langle \mathbf{u}' \cdot \nabla \times \mathbf{u}' \rangle \approx \langle u'_\theta \frac{\partial u'_\phi}{\partial r} \rangle. \quad (4)$$

This correlation function can be calculated provided that

$$\frac{\partial u'_\phi}{\partial r} \simeq \frac{\partial u'_\phi}{\partial t} \frac{1}{v_r}, \quad (5)$$

where  $v_r$  is the velocity for a rising flux tube. This may not be uniform over all depths, but in the first approximation we consider its variations small. With a constant  $v_r$  we may present the helicity with horizontal velocities and accelerations.

## 3. The data and methods

The data used here are presented in Paper I. Cycles 10 and 11 are covered by the Carrington and Spörer data (CS), and cycles 12 to 22 are covered by the GPR and SOON/NOAA data (GE).

The horizontal Reynolds stress is computed from two successive measurements of the same sunspot group in the following way: Firstly, the mean values  $\langle u_\theta \rangle$  and  $\langle u_\phi \rangle$  are computed. Secondly, from each velocity value the mean value is subtracted,

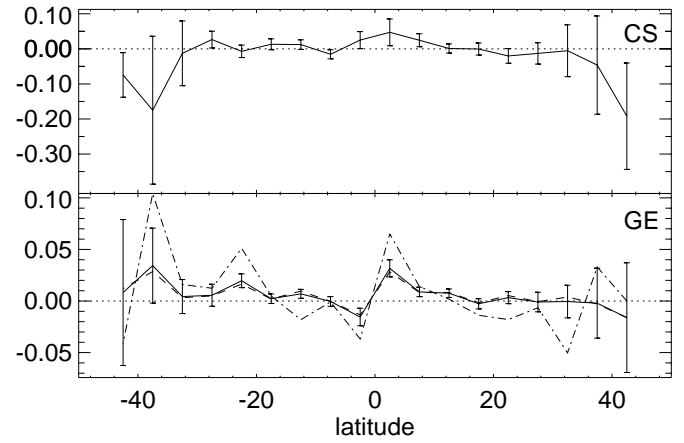


**Fig. 1.** Mean latitudinal velocity in units degrees/day for the CS data (upper panel) and GE data (lower panel). The continuous line with error bars denotes the full data. Also the latitudinal velocity of sunspot groups (dashed line) and single spots (dash-dotted line) are drawn for the GE data

giving  $u'_\theta = u_\theta - \langle u_\theta \rangle$  etc. Finally, the average  $\langle u'_\theta u'_\phi \rangle$  is computed. The concept of average deserves special attention here. The brackets  $\langle \rangle$  mean on the one hand temporal, and on the other hand spatial or other group averages. In other words, they define the bin in parameter space over which the average is taken.

## 4. Results

### 4.1. Latitudinal velocity

The mean motion along the meridians for the CS data and GE data (with sunspot groups and single spots separately) is plotted in Fig. 1. Here we consider the component  $u_\theta$  which is positive for southward velocities. A change of sign of  $u_\theta$  at the equator would be expected because of spherical symmetry. For the CS data,  $u_\theta$  does not seem to have any latitudinal dependence at all, and for the GE data, it is questionable whether we see the pattern of poleward flow at high ( $\gtrsim 15^\circ$ ) latitudes and equatorward at low latitudes. The equatorward motion is rather vague except in the very neighbourhood of the equator. This result is very similar to that of Ward (1965) and Balthasar et al. (1986). If we separate sunspot groups from single spots we see that single spots tend to have slightly larger poleward or equatorward motion than the rest of the data.

In many other sunspot studies as well, only a small latitudinal dependence has been found for  $u_\theta$ . On the other hand, results from magnetic tracers and Doppler shifts give very large poleward flows ( $\sim 10$  m/s) in both hemispheres (Komm et al. 1993) compared with our  $\sim 1$  m/s. Interestingly, the migration of the sunspot belt during a sunspot cycle has also a velocity of 1 m/s (30 degrees in 11 years), or 0.01 degrees/day. Moreover, it can be argued that the vague phenomenon presented above is just a statistical effect of the distribution of the sunspots. Averages taken in latitude bands may be incorrect due to the different densities of sunspots at different sides of the band. But if we

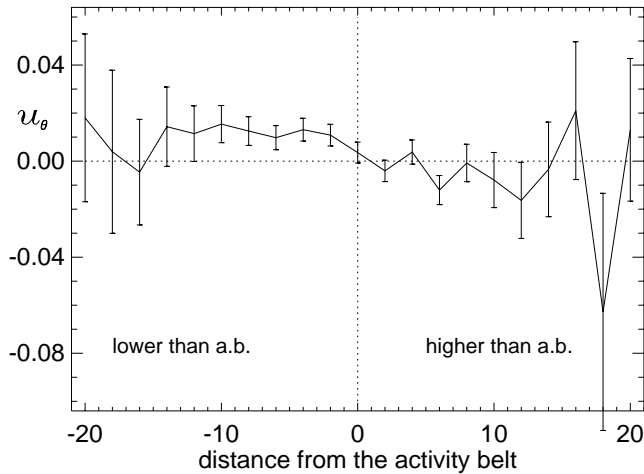


**Fig. 2.** Latitudinal velocity as a function of the distance from activity belt. The full data is considered, with those in southern hemisphere reflected to north. Positive distance in  $x$ -axis means higher latitude than the activity belt

exclude those velocity measurements resulting from sunspots at two neighbouring latitude bands, no essential differences to Fig. 1 are seen.

As was shown by J. Tuominen et al. (1983), the activity belt in the butterfly diagram is an important separator for latitudinal velocities. This can be seen in Fig. 2, in low latitudes the velocity is equatorward much more clearly than in Fig. 1. Therefore, to study further the qualitative behaviour of both the latitudinal velocity and Reynolds stress, we divide the both hemispheres in two bands. For latitudinal velocity, we use the activity belt as a dividing line, but for the Reynolds stress a more appropriate way is just to divide hemispheres in high and low latitudes. Table 1 lists results of these calculations in many subgroups.

In many cases the southward flows are stronger than the northward ones. For the GE data, for example, the northward flows vanish within error bars. However, throughout the subgroups, velocity values are small, less than 0.03 deg/day. If we persevere the idea of equatorward flow at low latitudes and poleward flow at high latitudes, the expected signs in the first four columns of Table 1 are  $-$ ,  $+$ ,  $-$ ,  $+$ . This “normal” behaviour is opposed in only five cases when the error bars are taken into account. The most significant of these occurs among youngest non-recurrent sunspots (see Paper I for the definition of these age groups). At higher latitudes than the activity belt these youngest sunspots have equatorward motion which might suggest that the youngest sunspots carry latitudinal flow in the opposite direction than the older sunspots.

At different cycles or cycle phases there is no clear development in the latitudinal velocities. But if we consider high and low bands as two pairs,  $u_\theta$  shows cycle phase behaviour which may not be random. In Fig. 3 we have plotted  $u_\theta$  vs. cycle phase in low latitude bands (panel a) and in high latitude bands (panel b). For those in bands in the southern hemisphere the sign has been changed because of the antisymmetry of  $u_\theta$ .

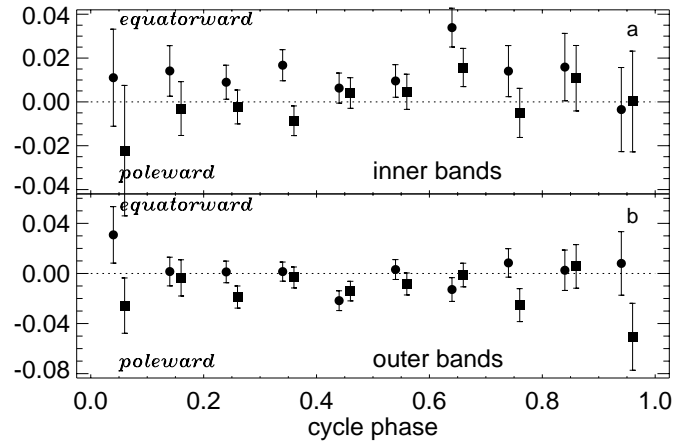


**Fig. 3.** Latitudinal velocity ( $u_\theta$ ) in units degrees/day at different cycle phases. In panel a,  $u_\theta$  of inner band N (circles) and  $-u_\theta$  of inner band S (squares) is shown. The  $x$ -axis of these two has been shifted to make the error bars readable. In addition, a dotted line is drawn to denote zero value, and the direction of the flow is written. In panel b there is  $u_\theta$  of outer band N (circles) and  $-u_\theta$  of outer band S (squares)

In bands closer to the equator  $u_\theta$  is strongly equatorward at descending phase ( $C_i = 7$ ) and more or less zero elsewhere. As for the outer bands,  $u_\theta$  is mostly poleward, especially at  $C_i = 4$ .

#### 4.2. The Reynolds stress

For both the CS and GE data, the latitudinal dependence of the Reynolds stress is shown in Fig. 4. The magnitude of  $Q_{\theta\phi}$  for both data sets is quite similar at the latitude range  $-25$  to  $25$  degrees. The crucial latitude for  $Q_{\theta\phi}$  is where the profile turns towards zero. On the basis of Fig. 4 this latitude may be at  $\pm 25$  degrees or over  $\pm 40$  degrees, when it is no longer observable from sunspot measurements. However, as shown by the dotted line in Fig. 4 indicating the number of measurements, the outermost values are very uncertain. Excluding them we get a profile that is supported also by computer simulations (Pulkkinen et al. 1993).

The behaviour of  $Q_{\theta\phi}$  shown above is qualitatively valid for almost all subgroups in the data. In Table 1 we give  $Q_{\theta\phi}$  in four latitude bands around the equator getting thus more information than just giving the  $w$ -coefficients of Eq. 3. This is because these coefficients are very sensitive to small changes of the latitudinal profile of  $Q_{\theta\phi}$ . Compared to the calculations of Ward (1965), we see that our results are slightly larger — about  $0.13$  (deg/day) $^2$  at high and about  $0.08$  (deg/day) $^2$  at low latitudes. These values are supported also by Gilman & Howard (1984) and Balthasar et al. (1986). However, the small or nonexistent  $Q_{\theta\phi}$  by Nesme-Ribes, et al. (1993) is puzzling.

As on rotation, the age of sunspots has an effect also on the Reynolds stress. Fig. 5 shows the development of  $Q_{\theta\phi}$  of aging sunspots. The error bars have been left out for clarity. Youngest sunspots possess largest  $Q_{\theta\phi}$  at nearly all latitudes. But qualitatively, all the profiles are similar and the turning point occurs at  $25$ - $30$  degrees in both hemispheres. Analogically with the

**Table 1.** Values of mean latitudinal velocity (left part) and horizontal Reynolds stress (right part) with their errors in various subgroups in four different latitude bands (see text)

no	latitudinal velocity ( $10^{-3}$ deg/day)				Reynolds stress ( $10^{-3}(\text{deg/day})^2$ )			
	high N	low N	low S	high S	$15^\circ\text{-}35^\circ$	$0^\circ\text{-}15^\circ$	$-15^\circ\text{-}0^\circ$	$-35^\circ\text{-}15^\circ$
full (GE)	$-3 \pm 3$	$13 \pm 3$	$-1 \pm 3$	$10 \pm 3$	$123 \pm 8$	$80 \pm 6$	$-71 \pm 6$	$-152 \pm 8$
full (CS)	$-2 \pm 12$	$7 \pm 10$	$0 \pm 9$	$9 \pm 11$	$111 \pm 45$	$100 \pm 38$	$-154 \pm 42$	$-175 \pm 41$
groups	$-1 \pm 4$	$12 \pm 3$	$1 \pm 3$	$9 \pm 4$	$134 \pm 9$	$87 \pm 7$	$-76 \pm 7$	$-163 \pm 9$
s/spots	$-17 \pm 6$	$20 \pm 7$	$-14 \pm 7$	$21 \pm 8$	$1 \pm 17$	$14 \pm 8$	$-21 \pm 13$	$-49 \pm 20$
nonrec	$-3 \pm 4$	$16 \pm 4$	$2 \pm 4$	$7 \pm 4$	$147 \pm 10$	$96 \pm 8$	$-85 \pm 9$	$-173 \pm 11$
recurr	$-2 \pm 4$	$7 \pm 4$	$-8 \pm 4$	$19 \pm 4$	$59 \pm 12$	$43 \pm 7$	$-38 \pm 6$	$-92 \pm 11$
max ph. (GE)	$-5 \pm 4$	$13 \pm 3$	$-1 \pm 3$	$10 \pm 4$	$114 \pm 9$	$79 \pm 7$	$-75 \pm 7$	$-157 \pm 9$
min ph. (GE)	$6 \pm 7$	$12 \pm 7$	$2 \pm 7$	$14 \pm 8$	$151 \pm 17$	$81 \pm 13$	$-55 \pm 15$	$-132 \pm 18$
max ph. (CS)	$-2 \pm 14$	$7 \pm 13$	$2 \pm 10$	$13 \pm 13$	$73 \pm 61$	$76 \pm 43$	$-144 \pm 46$	$-217 \pm 45$
min ph. (CS)	$-3 \pm 23$	$7 \pm 16$	$-7 \pm 19$	$-7 \pm 20$	$185 \pm 56$	$176 \pm 76$	$-187 \pm 99$	$-42 \pm 92$
ph.ind 0	$31 \pm 23$	$11 \pm 22$	$22 \pm 30$	$26 \pm 22$	$149 \pm 42$	$-31 \pm 48$	$-80 \pm 68$	$-69 \pm 37$
ph.ind 1	$2 \pm 11$	$14 \pm 12$	$3 \pm 12$	$4 \pm 14$	$156 \pm 21$	$56 \pm 49$	$88 \pm 120$	$-151 \pm 21$
ph.ind 2	$1 \pm 9$	$9 \pm 8$	$2 \pm 8$	$19 \pm 9$	$96 \pm 20$	$94 \pm 22$	$-118 \pm 26$	$-165 \pm 16$
ph.ind 3	$1 \pm 8$	$17 \pm 7$	$9 \pm 7$	$3 \pm 8$	$134 \pm 17$	$71 \pm 16$	$-67 \pm 16$	$-159 \pm 19$
ph.ind 4	$-22 \pm 8$	$6 \pm 7$	$-4 \pm 7$	$14 \pm 8$	$94 \pm 20$	$63 \pm 14$	$-78 \pm 15$	$-154 \pm 25$
ph.ind 5	$3 \pm 8$	$10 \pm 7$	$-5 \pm 8$	$8 \pm 9$	$126 \pm 19$	$85 \pm 15$	$-69 \pm 14$	$-136 \pm 23$
ph.ind 6	$-13 \pm 9$	$34 \pm 9$	$-16 \pm 9$	$1 \pm 9$	$150 \pm 32$	$94 \pm 14$	$-66 \pm 14$	$-151 \pm 26$
ph.ind 7	$8 \pm 11$	$14 \pm 12$	$5 \pm 11$	$25 \pm 13$	$159 \pm 39$	$103 \pm 17$	$-71 \pm 20$	$-152 \pm 72$
ph.ind 8	$3 \pm 16$	$16 \pm 15$	$-11 \pm 15$	$-6 \pm 17$	$120 \pm 109$	$99 \pm 28$	$-30 \pm 29$	$12 \pm 135$
ph.ind 9	$8 \pm 25$	$-4 \pm 19$	$0 \pm 23$	$51 \pm 27$	$12 \pm 167$	$25 \pm 36$	$-106 \pm 36$	$-198 \pm 87$
cycle 10	$-6 \pm 26$	$22 \pm 32$	$9 \pm 27$	$-28 \pm 29$	$35 \pm 147$	$206 \pm 104$	$-267 \pm 92$	$-289 \pm 80$
cycle 11	$18 \pm 23$	$29 \pm 28$	$-26 \pm 22$	$18 \pm 21$	$134 \pm 107$	$-64 \pm 115$	$-64 \pm 60$	$-40 \pm 133$
cycle 12	$-17 \pm 14$	$-4 \pm 11$	$-21 \pm 10$	$-12 \pm 12$	$76 \pm 25$	$59 \pm 23$	$-109 \pm 18$	$-163 \pm 27$
cycle 13	$18 \pm 14$	$21 \pm 10$	$15 \pm 9$	$25 \pm 11$	$258 \pm 33$	$73 \pm 18$	$-90 \pm 16$	$-221 \pm 36$
cycle 14	$-19 \pm 18$	$16 \pm 12$	$1 \pm 12$	$32 \pm 13$	$143 \pm 51$	$122 \pm 24$	$-51 \pm 22$	$-111 \pm 27$
cycle 15	$-8 \pm 10$	$12 \pm 7$	$-10 \pm 9$	$3 \pm 10$	$118 \pm 17$	$88 \pm 14$	$-35 \pm 19$	$-152 \pm 22$
cycle 16	$-5 \pm 8$	$4 \pm 8$	$-4 \pm 7$	$13 \pm 10$	$91 \pm 35$	$66 \pm 13$	$-56 \pm 16$	$-146 \pm 19$
cycle 17	$5 \pm 8$	$16 \pm 8$	$-5 \pm 8$	$12 \pm 8$	$134 \pm 20$	$43 \pm 14$	$-29 \pm 15$	$-138 \pm 17$
cycle 18	$-3 \pm 7$	$28 \pm 8$	$2 \pm 6$	$5 \pm 8$	$126 \pm 16$	$91 \pm 13$	$-73 \pm 13$	$-125 \pm 16$
cycle 19	$4 \pm 7$	$6 \pm 7$	$5 \pm 8$	$16 \pm 8$	$148 \pm 15$	$56 \pm 14$	$-50 \pm 16$	$-128 \pm 15$
cycle 20	$-20 \pm 9$	$1 \pm 8$	$-15 \pm 9$	$13 \pm 11$	$177 \pm 20$	$81 \pm 21$	$-70 \pm 20$	$-230 \pm 32$
cycle 21	$9 \pm 14$	$35 \pm 14$	$20 \pm 13$	$19 \pm 13$	$2 \pm 36$	$92 \pm 28$	$-88 \pm 30$	$-157 \pm 32$
cycle 22	$-11 \pm 15$	$0 \pm 14$	$-2 \pm 14$	$-7 \pm 14$	$121 \pm 31$	$106 \pm 38$	$-124 \pm 31$	$-138 \pm 39$
youngest nrc	$21 \pm 13$	$33 \pm 12$	$0 \pm 12$	$5 \pm 13$	$190 \pm 31$	$87 \pm 25$	$-54 \pm 28$	$-235 \pm 33$
youngest rec	$10 \pm 28$	$-11 \pm 23$	$-3 \pm 30$	$8 \pm 26$	$159 \pm 51$	$89 \pm 44$	$-91 \pm 60$	$-139 \pm 46$
young nrc	$-3 \pm 9$	$15 \pm 8$	$0 \pm 8$	$0 \pm 9$	$164 \pm 23$	$104 \pm 16$	$-118 \pm 17$	$-175 \pm 23$
young rec	$2 \pm 13$	$24 \pm 12$	$-30 \pm 11$	$18 \pm 12$	$82 \pm 18$	$73 \pm 18$	$-43 \pm 15$	$-111 \pm 23$
old nec	$-8 \pm 5$	$12 \pm 5$	$3 \pm 5$	$11 \pm 5$	$128 \pm 12$	$93 \pm 10$	$-78 \pm 11$	$-157 \pm 13$
old rec	$-1 \pm 6$	$5 \pm 6$	$-14 \pm 6$	$28 \pm 7$	$64 \pm 9$	$33 \pm 7$	$-40 \pm 6$	$-44 \pm 9$
oldest	$-5 \pm 6$	$7 \pm 6$	$0 \pm 5$	$15 \pm 6$	$40 \pm 20$	$41 \pm 10$	$-30 \pm 10$	$-109 \pm 18$

assumption of the “anchoring-effect” of young sunspots (discussed in Paper I) we can interpret this result by saying that deeper layers are more efficient in transporting angular momentum than upper layers.

The Reynolds stress profiles of sunspot groups and single spots differ largely with each other. As the maximum correlation in the GE data for sunspot groups is about  $0.27 (\text{deg/day})^2$  for single spots it hardly reaches  $0.04 (\text{deg/day})^2$ , i.e. only 15% of that of groups. It has been pointed out by Leighton (unpublished, see Gilman & Howard, 1984) that the apparent Reynolds stress of sunspot groups is at least mostly due to their changes in shape in the course of time. Since single spots are more regularly shaped they should yield a more reliable Reynolds stress

profile than groups. However, as we can see in Table 3 of Paper I and Fig. 1, single spots rotate slower and perhaps have larger latitudinal velocity than sunspot groups. The former result can be interpreted by saying that single spots are representatives of older sunspots and therefore slower than average sunspot groups. From this we can expect that the Reynolds stress of single spots is of the same order of magnitude as old sunspot groups. In fact,  $Q_{\theta\phi}$  for single spots is even smaller than that of oldest sunspots (Fig. 5) so the above cannot be the whole truth. Another explanation may lie in the different motion of single spots compared to sunspot groups. Bray & Loughhead (1965, p.231) describe the proper motions of preceding and following single spots, and what can be decided is that the net effect in

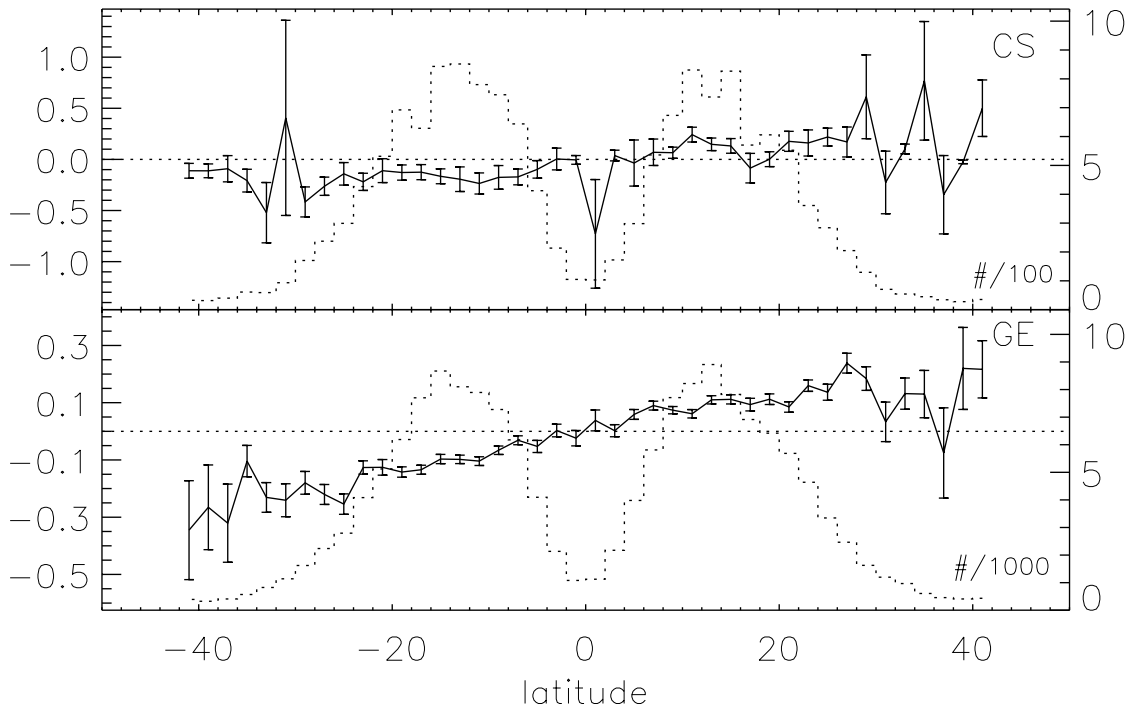


**Fig. 4.** The horizontal Reynolds stress  $Q_{\theta\phi}$  for the CS and GE data. The dashed lines are show the numbers of measurements in hundreds (thousands) of the CS (GE) data

differential rotation may well be slower and latitudinal motion more equatorward than that of sunspot groups. Also, the change in direction of proper motion of preceding spots may result in a small Reynolds stress.

The long-time development of the horizontal Reynolds stress can be studied when different cycles are considered separately. We plot the average Reynolds stress in both hemispheres for each cycle in Fig. 6. The behaviour of  $Q_{\theta\phi}$  between hemispheres is almost symmetric during cycles 13, 15-20, and 22 but deviates quite much at other cycles. No clear correlation can be seen between the magnitude of  $Q_{\theta\phi}$  and the cycle activity. On the contrary,  $Q_{\theta\phi}$  seems to be almost constant throughout the cycles.

Also in the course of a cycle,  $Q_{\theta\phi}$  remains almost constant, although this behaviour is more consistent in the maximum phase. During minimum phase, fluctuations are larger, and sometimes  $Q_{\theta\phi}$  even has the “wrong” sign. In different age groups we do not find significant difference between these two phases except for the oldest sunspots where they lack  $Q_{\theta\phi}$  in minimum phase. From this we cannot say that the Reynolds stress would substantially depend on the current state of the magnetic field.

### 4.3. Helicity

To calculate the helicity  $H$  (RHS of Eq. 4) of the fluctuation velocity field we need the radial derivative of the angular velocity. This is accomplished by taking the difference between two successive velocity values and dividing it by the time difference.

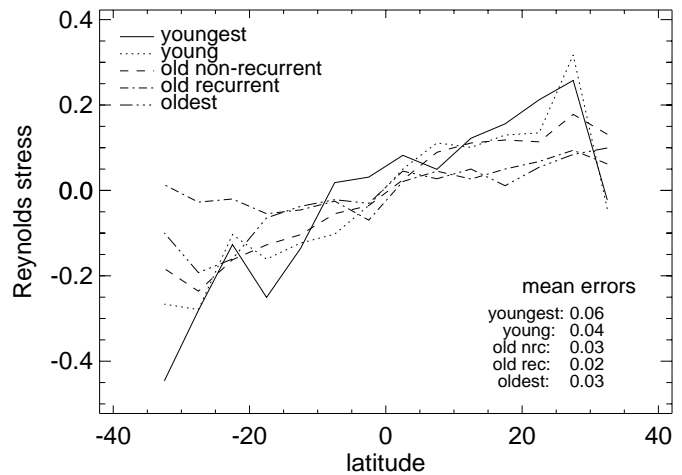


**Fig. 5.**  $Q_{\theta\phi}$  for the five reference age groups

It was shown in Paper I that a detectable gradient of angular velocity can be obtained only for sunspots younger than a week. Thus, we do not find it surprising that  $H$  is practically 0 when we consider the entire data or each cycle separately. The situation does not change much, if we look at different age groups and/or smaller time scales. Some deviations from zero are seen but they are not statistically important. We may conclude that the helicity of the turbulent motions is not obtainable from this data.

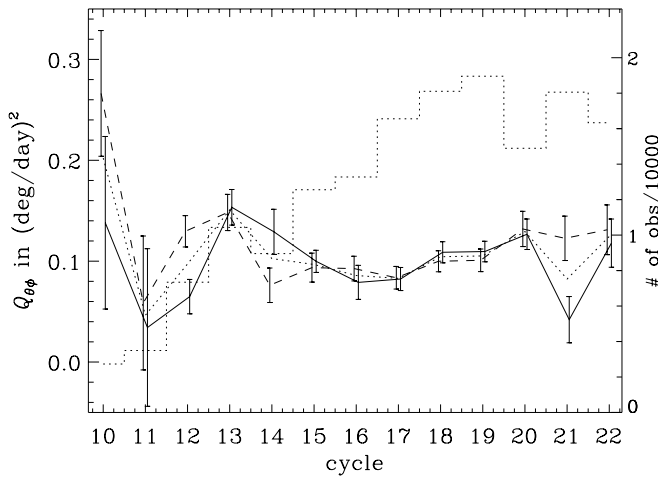


**Fig. 6.** The horizontal Reynolds stress  $Q_{\theta\phi}$  at cycles 10 to 20 in the northern (solid line) and southern (dashed line) hemisphere. The sign of  $Q_{\theta\phi}$  at the south has been changed. The dotted line shows the total average of  $Q_{\theta\phi}$  and the histogram line denotes the number of observations of each cycle

## 5. Conclusions and discussion

Latitudinal velocity is much more difficult to handle than rotation because the mean flow is so weak if existent at all. In fact, the origin of latitudinal flow in Fig. 1 may not be fully answered on the basis of this work. Usually this flow is considered to be large-scale meridional circulation carrying angular momentum, a hint of which is also seen through the opposite flow of youngest sunspots. However, another possible source for this flow is the activity belt. We have pointed out the phase dependence of latitudinal flow in latitude bands 1 to 4 (Figs. 3a and 3b) which vanishes without this band division. On this basis it would seem more probable that the band separating equatorward and poleward flows is moving rather than staying at the same latitude in the course of the cycle, which was proposed also by J. Tuominen et al. (1983).

As was pointed out by Balthasar and Wöhl (1980) and Howard et al. (1984), an interesting feature in the latitudinal flow is the much larger southward flow compared to the northward ones, even if cycles are separated. This is hardly a real effect at least totally, but it may give a hint of a large global circulation.

The possibility of measuring also the Reynolds stress from sunspot observations has been questioned by some authors. However, we think that the latitudinal profile shown in Fig. 4 is a true phenomenon and the small Reynolds stress in single spots is due to their older age and more importantly, different proper motion. Therefore, we may add that deep parts of the convection zone are more efficient in transporting angular momentum than higher layers. It is not clear, however, whether the turning point of  $Q_{\theta\phi}$  (Fig. 4) really occurs at  $\pm 25$  degrees or does the strange behaviour at high latitudes have any relevance. Therefore, it may never be possible to obtain a better view for the Reynolds stress from sunspot measurements.

The magnitude of  $Q_{\theta\phi}$  derived here show that the Reynolds stress is really an important and efficient transporter on angular momentum. From the results of Table 1 it is obvious that the horizontal Reynolds stress is present at all photospheric motions provided that sunspots are reliable tracers of such motions.

Helicity of the small-scale velocity does not show a systematic behaviour. Only for the youngest sunspots in the most active cycles are we able to see deviation from random noise. But then  $H$  is more or less symmetric with respect to the equator, contrary to what one would expect. The main reason for poor results for helicity is definitely due to computational difficulties. Although the radial gradient of mean rotation could be presented quite reliably, we would need the fluctuation of that gradient which is statistically uncertain.

*Acknowledgements.* PP thanks JILA for their hospitality during his stay. This work belongs to the EC Human Capital and Mobility (Networks) project “Late type stars: activity, magnetism, turbulence” No. ERBCHRXCT940483.

## References

- Balthasar, H., Vázquez, M., Wöhl, H.: 1986, *A&A* 155, 87  
 Balthasar, H., Wöhl, H.: 1980, *A&A* 92, 111  
 Bray, R.J., Loughhead, R.E.: 1965, *Sunspots*, Wiley, New York  
 Carrington, R.C.: 1863, *Observations of the spots of the sun*, London  
 Canuto, V.M., Minotti, F.O., Schilling, O.: 1994, *ApJ* 425, 303  
 Gilman, P.A., Howard, R.: 1984, *Solar Phys.* 93, 171  
 Howard, R., LaBonte, B.J.: 1980, *ApJ* 239, L33  
 Howard, R., Gilman, P.A.: 1986, *ApJ* 307, 389  
 Howard, R., Gilman, P.A., Gilman, P.I.: 1984, *ApJ* 283, 373  
 Komm, R.W., Howard, R.F., Harvey, J.W.: 1993, *Solar Phys.* 147, 207  
 Krause, F., Rädler, K.-H.: 1980, *Mean-field magnetohydrodynamics and dynamo theory*, Akademie-Verlag, Berlin  
 Nesme-Ribes, E., Ferreira, E.N., Vince, I.: 1993, *A&A* 276, 211  
 Paternò, L., Spadaro, D., Zappalà, R.A., Zuccarello, F.: 1991, *A&A* 252, 337  
 Pulkkinen, P., Tuominen, I., Brandenburg, A., Nordlund, Å., Stein, R. F.: 1993, *A&A* 267, 265  
 Royal observatory, Greenwich: 1874-1976, *Greenwich Photoheliographic Results*, in 103 volumes  
 Rüdiger, G.: 1980, *GAFD* 16, 239  
 Rüdiger, G., Tuominen, I., Krause, F., Virtanen, H.: 1986, *A&A* 166, 306  
 Spörer, G.: 1878, *Publ. Astrophys. Obs. Potsdam*, 1, 1  
 Spörer, G.: 1880, *Publ. Astrophys. Obs. Potsdam*, 2, 1  
 Spörer, G.: 1886, *Publ. Astrophys. Obs. Potsdam*, 4, 217  
 Spörer, G.: 1884, *Publ. Astrophys. Obs. Potsdam*, 10, 1  
 Tuominen, J.: 1941, *Z. Astrophys.* 21, 96  
 Tuominen, J., Kyröläinen, J.: 1982, *Solar Phys.* 79, 161  
 Tuominen, J., Tuominen, I., Kyröläinen, J.: 1983, *MNRAS* 205, 691  
 Ward, F.: 1965, *ApJ* 141, 534  
 Ward, F.: 1973, *Solar Phys.* 30, 527